Hindawi
Journal of Advanced Transportation
Volume 2023, Article ID 9895680, 1 page
https://doi.org/10.1155/2023/9895680

Retraction

Retracted: Statistical Characteristics and Security Analysis over Multi-Cascade κ-μ Shadowed Channels

Journal of Advanced Transportation

Received 19 December 2023; Accepted 19 December 2023; Published 20 December 2023

This article has been retracted by Hindawi following an investigation undertaken by the publisher [1]. This investigation has uncovered evidence of one or more of the following indicators of systematic manipulation of the publication process:

(1) Discrepancies in scope

(2) Discrepancies in the description of the research reported

(3) Discrepancies between the availability of data and the research described

(4) Inappropriate citations

(5) Incoherent, meaningless and/or irrelevant content included in the article

(6) Manipulated or compromised peer review

The presence of these indicators undermines our confidence in the integrity of the article's content and we cannot, therefore, vouch for its reliability. Please note that this notice is intended solely to alert readers that the content of this article is unreliable. We have not investigated whether authors were aware of or involved in the systematic manipulation of the publication process.

Wiley and Hindawi regrets that the usual quality checks did not identify these issues before publication and have since put additional measures in place to safeguard research integrity.

We wish to credit our own Research Integrity and Research Publishing teams and anonymous and named external researchers and research integrity experts for contributing to this investigation.

The corresponding author, as the representative of all authors, has been given the opportunity to register their agreement or disagreement to this retraction. We have kept a record of any response received.

References

[1] X. Wang, M. Ren, Y. Fang, X. Tian, and Y. Zeng, "Statistical Characteristics and Security Analysis over Multi-Cascade κ-μ Shadowed Channels," *Journal of Advanced Transportation*, vol. 2022, Article ID 5342655, 10 pages, 2022.

Hindawi
Journal of Advanced Transportation
Volume 2022, Article ID 5342655, 10 pages
https://doi.org/10.1155/2022/5342655

Research Article

Statistical Characteristics and Security Analysis over Multi-Cascade κ-μ Shadowed Channels

Xiaohong Wang,[1] **Ming Ren**,[2] **Yiwei Fang**,[3] **Xinji Tian**,[1] **and Yanyang Zeng**[4]

[1]*The College of Physics and Electronic Information Engineering, Henan Polytechnic University, Jiaozuo 454003, China*
[2]*The Department of Mathematics and Physics Education, Luoyang Institute of Science and Technology, Luoyang 471023, China*
[3]*The Wuhan Maritime Communication Research Institute, Wuhan 430079, China*
[4]*The College of Computer Science and Technology, Henan Polytechnic University, Jiaozuo 454003, China*

Correspondence should be addressed to Ming Ren; renming926@163.com

Received 24 March 2022; Revised 10 May 2022; Accepted 16 May 2022; Published 20 June 2022

Academic Editor: Li Feng

In this paper, the statistical characteristics of the multi-cascade κ-μ shadowed fading channels are investigated and analyzed under the classic Wyner's eavesdropping model. In particular, the general accurate expressions of the probability density function and the cumulative distribution function for amplitude and signal-to-noise ratio (SNR) are derived for the first time. Moreover, we further utilize the two performance evaluation metrics including outage probability and intercept probability to investigate the impacts of cascade number and channel parameters on reliability and security. Finally, the theoretical results are consistent with the simulations, proving the correctness of the derivation. The interesting conclusion is that when the average SNR is greater than 2 dB, the reliability of the multi-cascade model will decrease as the number of cascade increases; on the contrary, more cascading can lead to stronger anti-eavesdropping ability.

1. Introduction

With the wide application of wireless networks, people have higher demands on the transmission performance and security of the communication system. Secure and reliable wireless communication systems have become an important support for providing reliable services, transmitting confidential information, ensuring social stability, and maintaining national security. Different from traditional encryption and decryption algorithms, physical layer security (PLS) utilizes its fading properties to improve the system's anti-eavesdropping ability by increasing the security capacity. Many scholars are committed to the security performance analysis of communication networks and have obtained some research results [1–8]. Wyner et al. in [1] proposed the security matter of the physical layer. The most crucial feature of physical security was to use the characteristics of its own channel to evaluate and improve the anti-eavesdropping capabilities of the system [2]. The authors in [3] utilized the collaborative automatic repeat request technology to improve the security performance. Cao et al. in [4] studied the PLS of the collaborative non-orthogonal multiple access (NOMA) system. The authors in [5] evaluated the confidentiality of cognitive radio networks. Song et al. in [6] investigated the optimal confidentiality capabilities of two different schemes of amplified forwarding and coordinated interference based on cooperative communication. The basic metrics on physical layer performance over fading distributions were defined and researched in [7, 8], such as the strictly positive secrecy capacity (SPSC), the security outage probability (SOP), and the average secrecy capacity (ASC).

In practical wireless communication systems, wireless fading channels are susceptible to noise, interference, and other channel factors, which can lead to serious challenges for reliable communication. Therefore, research on fading channels is of great practical significance. The statistical characteristics of the channel are crucial to the analysis of

system performance [9]. In recent years, with the emergence of complex communication environments, many fading channels have been explored by scholars [10–18]. When there is no line-of-sight component in the transmitted signal, the fading channel can be modeled as Rayleigh distribution [10]. Mason et al. in [11] put forward the Rician fading, which is also called Nakagami-n distribution. The Nakagami-m fading was first studied in [12], and its statistical properties were investigated in [13]. The η-μ fading can characterize small-scale changes of fading signals [14], and the accurate expression of the level crossing rate was investigated. Michel et al. in [15] proposed the α-μ distribution and deduced the principal characteristic function of the channels. The authors in [16] applied α-μ fading to the NOMA system and analyzed the effect of residual transceiver hardware impairments on the communication networks. The κ-μ fading considers the propagation of signal in a nonuniform scene, and the authors in [17] gave the characteristics of κ-μ fading distribution and important attributes. Imperfect Weibull channels and their applications were researched in [18].

The above-mentioned channels are all single-fading channels, but in practice, many scenarios are more complex and need to be simulated by complicated models. For example, since the mobile-to-mobile communication model experienced more severe channel fading, the cascaded Nakagami-m distribution model was used to simulate this scenario [19]. The cascaded fading channel can also be applied to satellite communications systems [20], ultra-high frequency identification systems [21], multiple-input multiple-output correspondence [22], and vehicle-to-vehicle communication networks [23]. Therefore, more and more research on n-level cascaded fading channels has been conducted in recent years [24–26]. The precise expressions of the probability density function (PDF) and cumulative distribution function (CDF) for the SNR of the $N*$ Nakagami random variables were first investigated in [24]. The cascaded Weibull distribution was composed of multiple random variables, and its statistical properties were derived in [25]. Tashman et al. in [26] studied the expressions of PDF and CDF of the receivers' SNR of the multi-cascade κ-μ distribution and deduced security performance of the channels when there are multiple eavesdroppers.

The κ-μ fading is a general composite distribution, which can be simplified to Rician, Nakagami-m, and Rayleigh models by changing the parameters [17] where as the channel assumes that the components in each cluster are deterministic. For the limitation of κ-μ distribution, the κ-μ shadowed distribution was first investigated in [27], which is the physical extension of the κ-μ fading. The channel can simulate that the deterministic components of all clusters fluctuate stochastically. Also, the accurate expressions of PDF and CDF of SNR over the κ-μ shadowed distribution have been obtained, which makes it easier to carry out mathematical operations and analyses. The security of κ-μ shadowed fading was analyzed in [28], and the precise expressions of SPSC and the lower limit of SOP were investigated. The authors in [29] gave the capacity analysis of the multiple-input multiple-output communication system over κ-μ shadowed distribution. The security performance of downlink NOMA networks over κ-μ shadowed fading was researched in [30]. Bhatnagar in [31] studied the statistical properties of correlated squared κ-μ shadowed fading by deriving theoretical expressions for PDF and moment-generating function. In [32], the outage probability (OP) of amplify-and-forward relay communication system over κ-μ shadowed distribution and the expression of ASC were studied; moreover, the effect of beamforming and shaping arguments on system property was analyzed. Sun et al. in [33] deduced the new expression of SOP for single-input multi-output system based on the κ-μ shadowed random variables. In [34], the authors investigated the effective rate of communication networks under κ-μ shadowed random variables. The authors in [35] deduced the theoretical formulas of the channel capacity over κ-μ shadowed fading and investigated the performance of the spectrum aggregation system based on composite fading channels.

References [1–8] describe the research on wireless communication network security by scholars, references [9–18] mainly list the investigation status of several common fading channels, references [19–26] aim to present the cascaded wireless related investigations and applications of fading channels, and references [19–34] specifically introduce the characteristics and research status of the κ-μ shadowed random variables. Combining the above analysis, to the authors' knowledge, no relevant literature exploring multi-cascaded κ-μ shadowed distribution has appeared in the current database. Therefore, we carried out this work. Furthermore, the outstanding contributions of the paper are summarized as follows:

(1) Through the statistical analysis, the accurate expression of PDF and CDF of SNR over a multi-cascaded model is deduced mainly by deriving the unified closed expression of PDF and CDF of the amplitude of n-level κ-μ shadowed distribution.

(2) Based on the derived expressions of PDF and CDF of SNR, the theoretical analytic equations of OP and intercept probability (IP) are derived, and the security performance of the system is analyzed. Finally, the theoretical results and Monte Carlo simulations are used for comparison and verification. Moreover, the impacts of its parameters on the systems' performance are discussed.

The content of the paper is arranged as follows. Section 2 depicts the system model and statistical features. Section 3 derives the universal formulas for PDF and CDF of amplitude and SNR under the multi-cascade κ-μ shadowed distribution. The theoretical expressions of OP and IP are presented in Section 4. The influences of each parameter are provided in Section 5. The conclusions of this paper are given in Section 6.

2. System Model and Channel Characteristics

2.1. System Model. In Figure 1, the paper considers Wyner's eavesdropping model under multi-cascade κ-μ shadowed fading. The model mainly includes an emission source (S), a

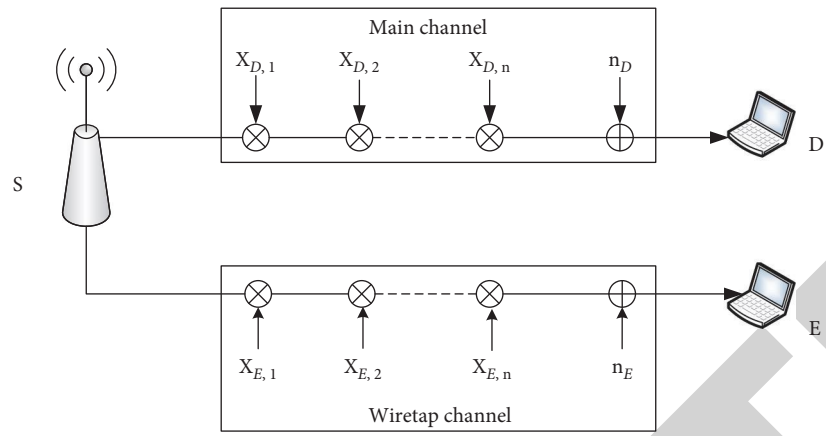

Figure 1: The system model.

legitimate user (D), and an illegal user (E). We suppose that confidential information is transmitted through the main channel (S to D), but the eavesdropper will intercept the information through the eavesdropping channel (S to E). The fading of both the main (S to D) and wiretap (S to E) channels experiences multi-cascade κ-μ shadowed distribution, where $X_{D,i}$ and $X_{E,i}$, $i \in \{1, n\}$ represent the i-th cascade channel gain of the main channel and the eavesdropping channel, respectively.

The signal received by the receiving terminals (D or E) can be expressed as

$$y_w = h_w x + n_w \quad w \in \{D, E\}, \tag{1}$$

where x denotes the transmitting signal and n_w represents the additive white Gaussian noise (AWGN) with an average value of zero and fixed variance σ_n^2. In addition, h_w represents multi-cascade κ-μ shadowed distributions between S and w, which can be expressed as

$$h_w = \prod_{i=1}^{n} h_{w,i}, \tag{2}$$

where $h_w = \prod_{i=1}^{n} h_{w,i}$ is the product of amplitudes representing κ-μ shadowed fading with the independent non-identical distribution.

2.2. Statistical Features. We presume that both the main and eavesdropper channels are submissive to i.n.i.d. over κ-μ shadowed random variables, and the PDF of the SNR over the channel was presented as [27]

$$f_\gamma(\gamma) = \frac{m^m (1+\kappa)^\mu \mu^\mu}{\Gamma(\mu)(m+\kappa\mu)^m \overline{\gamma}} \left(\frac{\gamma}{\overline{\gamma}}\right)^{\mu-1} e^{-\gamma(1+\kappa)\mu/\overline{\gamma}} \times {}_1F_1\left(m; \mu; \frac{\mu^2 \kappa (1+\kappa)\gamma}{\overline{\gamma}(m+\kappa\mu)}\right), \tag{3}$$

where $\kappa = d^2/2\sigma^2\mu$, d^2 indicates total power of primary ingredients, $2\sigma^2\mu$ represents the general power of scattered waves, $\kappa > 0$ represents the ratio of aggregate power of the primary ingredients to the overall power of the dispersive waves, and $\mu > 0$ is an attenuation parameter whose value is correlative to the quantity N of cluster groups in the received signal. M is the shaping parameter of Nakagami-m distribution. Besides, $\overline{\gamma} = E[\cdot]$ and $E[\cdot]$ represent the average SNR and the expectation operator, respectively. $\Gamma(\cdot)$ is defined in [36, eq. (8.310.1)] and ${}_1F_1(\cdot)$ is contained in [36, eq. (9.210.1)].

The PDF of the amplitude for single κ-μ shadowed random variable was deduced as [37]

$$f_X(x) = \frac{2m^m (1+\kappa)^\mu \mu^\mu}{\Gamma(\mu)(m+\kappa\mu)^m} \frac{x^{2\mu-1}}{\Omega^\mu} e^{-x^2(1+\kappa)\mu/\Omega} \times {}_1F_1\left(m; \mu; \frac{\mu^2 \kappa (1+\kappa) x^2}{\Omega(m+\kappa\mu)}\right), \tag{4}$$

where $\Omega = E[R^2]$ represents the mean power and $E[R^2] = 2\mu\sigma^2 + d^2$ is the average signal power.

3. System Model and Channel Characteristics

This section mainly deduces the theoretical expressions of the PDF and CDF for amplitude and SNR over multi-cascade κ-μ shadowed fading.

3.1. Analysis of Channel Amplitude Characteristics. The amplitude of κ-μ shadowed fading with cascade degree n is expressed as

$$Y_n = \prod_{i=1}^{n} X_i, \tag{5}$$

where $Y_n = \prod_{i=1}^{n} X_i$ is the transformation of (2). Since the derivation process of the main and the eavesdropping channels is similar, only the main channel is considered in the analysis. Also, we denote the product of the magnitude of the cascade by $\{X_i\}_{i=1}^{n}$.

We first consider the condition of the two-level cascade. Let $Y_2 = X_1 X_2$; these two random variables are considered the product of the PDF of X_1 and X_2 of κ-μ shadowed fading. Employing substitution of random variables, the PDF of Y_2 is represented by the following equation:

$$f_{Y_2}(y) = \int_{-\infty}^{\infty} \frac{1}{|t|} f_{X_1}\left(\frac{y}{t}\right) f_{X_2}(t)\mathrm{d}t. \tag{6}$$

Substituting (4) into (6),(6) can be rewritten as

$$f_{Y_2}(y) = \Phi_1 y^{2\mu_1-1} \int_0^{\infty} t^{-2\mu_1+2\mu_2-1} \times \exp\left(-\frac{(y/t)^2(1+\kappa_1)\mu_1}{\Omega_1}\right) \times \exp\left(-\frac{(t)^2(1+\kappa_2)\mu_2}{\Omega_2}\right) \times {}_1F_1\left(m_1;\mu_1;\frac{\mu_1^2\kappa_1(1+\kappa_1)(y/t)^2}{\Omega_1(m_1+\kappa_1\mu_1)}\right) \times {}_1F_1\left(m_2;\mu_2;\frac{\mu_2^2\kappa_2(1+\kappa_2)(t)^2}{\Omega_2(m_2+\kappa_2\mu_2)}\right)\mathrm{d}t, \tag{7}$$

where Φ_1 is given as

$$\Phi_1 = \frac{2m_1^{m_1}(1+\kappa_1)^{\mu_1}\mu_1^{\mu_1}}{\Gamma(\mu_1)(m_1+\kappa_1\mu_1)^{m_1}} \frac{1}{\Omega^{\mu_1}} \times \frac{2m_2^{m_2}(1+\kappa_2)^{\mu_2}\mu_2^{\mu_2}}{\Gamma(\mu_2)(m_2+\kappa_2\mu_2)^{m_2}} \frac{1}{\Omega^{\mu_2}}. \tag{8}$$

After some mathematical operations, (7) can be rewritten as

$$f_{Y_2}(y) = \sum_{g_1=0}^{\infty}\sum_{g_2=0}^{\infty} \frac{\Phi_1\Phi_2}{2} y^{2\mu_1+2g_1-1} \times \left[\frac{(1+\kappa_2)\mu_2}{\Omega_2}\right]^{\mu_1-\mu_2+g_1-g_2} \times G_{2,0}^{0,2}\left[\frac{\Omega_1\Omega_2}{(1+\kappa_1)\mu_1(1+\kappa_2)\mu_2 y^2}\middle|\begin{matrix}1, 1+\mu_1-\mu_2+g_1-g_2\\ -\end{matrix}\right], \tag{9}$$

where

$$\Phi_2 = \frac{(m_1)_{g_1}}{(\mu_1)_{g_1} g_1!}\left[\frac{\mu_1^2\kappa_1(1+\kappa_1)}{\Omega_1(m_1+\kappa_1\mu_1)}\right]^{g_1} \times \frac{(m_2)_{g_2}}{(\mu_2)_{g_2} g_2!}\left[\frac{\mu_2^2\kappa_2(1+\kappa_2)}{\Omega_2(m_2+\kappa_2\mu_2)}\right]^{g_2}. \tag{10}$$

Through mathematical induction, the PDF of multi-cascade κ-μ shadowed distribution can be written as

$$f_{Y_n}(y) = \sum_{g_1=0}^{\infty}\sum_{g_2=0}^{\infty}\cdots\sum_{g_{n=0}}^{\infty} \Phi_x y^{2\mu_1+2g_1-1} \times G_{n,0}^{0,n}\left[\frac{\prod_{i=1}^{n}\Omega_i}{y^2\prod_{i=1}^{n}(1+\kappa_i)\mu_i}\middle|\begin{matrix}\Psi\\ -\end{matrix}\right], \tag{11}$$

where $\psi = 1, 1+\mu_1-\mu_2+g_1-g_2, \ldots, 1+\mu_1-\mu_n+g_1-g_n$ and

$$\Phi_x = 2\prod_{i=1}^{n} \frac{m_i^{m_i}(1+\kappa_i)^{\mu_i}\mu_i^{\mu_i}}{\Gamma(\mu_i)(m_i+\kappa_i\mu_i)^{m_i}} \left(\frac{1}{\Omega_i}\right)^{\mu_1+g_1} \times \prod_{i=1}^{n}\left[(1+\kappa_i)\mu_i\right]^{\mu_1-\mu_i+g_1-g_i} \times \prod_{i=1}^{n} \frac{(m_i)_{g_i}}{(\mu_i)_{g_i} g_i!}\left[\frac{\mu_i^2\kappa_i(1+\kappa_i)}{(m_i+\kappa_i\mu_i)}\right]^{g_i}. \tag{12}$$

After some operations, the CDF of amplitude can be obtained as

$$F_{Y_n}(y) = \sum_{g_1=0}^{\infty}\sum_{g_2=0}^{\infty}\cdots\sum_{g_{n=0}}^{\infty} \Phi_x \int_0^{y} x^{2\mu_1+2g_1-1} \times G_{n,0}^{0,n}\left[\frac{\prod_{i=1}^{n}\Omega_i}{x^2\prod_{i=1}^{n}(1+\kappa_i)\mu_i}\middle|\begin{matrix}\Psi\\ -\end{matrix}\right]\mathrm{d}x. \tag{13}$$

According to [38], we have

$$\int_0^{y} x^{\alpha-1} G_{u,v}^{s,t}\left[\omega x\middle|\begin{matrix}(a_u)\\ (b_v)\end{matrix}\right]\mathrm{d}x = y^{\alpha} G_{u+1,v+1}^{s,t+1}\left[\omega y\middle|\begin{matrix}a_1,\ldots,a_t,1-\alpha,a_t,\ldots,a_u\\ b_1,\ldots,b_s,-\alpha,b_{s+1},\ldots,b_v\end{matrix}\right], \tag{14}$$

and using (A.5) and (14), formula (13) can be converted to

$$F_{Y_n}(y) = \sum_{g_1=0}^{\infty}\sum_{g_2=0}^{\infty}\cdots\sum_{g_n=0}^{\infty}\frac{\Phi_x}{2}y^{2(\mu_1+g_1)} \times G_{1,n+1}^{n,1}\left[\frac{\prod_{i=1}^{n}(1+\kappa_i)\mu_i}{\prod_{i=1}^{n}\Omega_i}y^2\middle|\begin{matrix}1-\mu_1-g_1\\ \zeta\end{matrix}\right], \tag{15}$$

where.
$\zeta = 0, -\mu_1+\mu_2-g_1+g_2,\ldots,-\mu_1+\mu_n-g_1+g_n,-\mu_1-g_1$.

Proof. See Appendix. □

3.2. Characteristics Analysis of SNR. This section will give the PDF and CDF of the SNR. We utilize the variate γ to represent the SNR at the import of the receiving terminal. The received average SNR ($\overline{\gamma}$) is expressed as

$$\overline{\gamma} = E\left[Y_n^2\right]\frac{P}{N_0}, \tag{16}$$

where Y_n is the product vector of the multi-cascade κ-μ shadowed fading, N_0 is the power spectral density of AWGN, and P is the transmitted power. Using (5) and (16), we can obtain

$$\overline{\gamma} = \frac{P}{N_0}\prod_{i=0}^{n}E\left[X_i^2\right]. \tag{17}$$

According to [10, eq. (2.3)], the PDF of the SNR at receiver terminal can be written as

$$f_\gamma(\gamma) = \frac{f_{Y_n}\left(\sqrt{\prod_{i=0}^{n}\Omega_i\gamma/\overline{\gamma}}\right)}{2\sqrt{\gamma\overline{\gamma}/\prod_{i=0}^{n}\Omega_i}}. \tag{18}$$

Substituting (11) into (18),

$$f_\gamma(\gamma) = \sum_{g_1=0}^{\infty}\sum_{g_2=0}^{\infty}\cdots\sum_{g_n=0}^{\infty}\frac{\Lambda_x}{2}\left(\frac{1}{\overline{\gamma}}\right)^{\mu_1+g_1} \times G_{n,0}^{0,n}\left[\frac{\overline{\gamma}}{\gamma\prod_{i=1}^{n}(1+\kappa_i)\mu_i}\middle|\begin{matrix}\Psi\\ -\end{matrix}\right]\gamma^{\mu_1+g_1-1}. \tag{19}$$

By using (A.5) and (14), the CDF of SNR can be gained as

$$F_\gamma(\gamma) = \sum_{g_1=0}^{\infty}\sum_{g_2=0}^{\infty}\cdots\sum_{g_n=0}^{\infty}\frac{\Lambda_x}{2}\left(\frac{\gamma}{\overline{\gamma}}\right)^{\mu_1+g_1} \times G_{1,n+1}^{n,1}\left[\frac{\prod_{i=1}^{n}(1+\kappa_i)\mu_i}{\overline{\gamma}}\gamma\middle|\begin{matrix}1-\mu_1-g_1\\ \zeta\end{matrix}\right], \tag{20}$$

where

$$\Lambda_x = 2\prod_{i=1}^{n}\frac{m_i^{m_i}(1+\kappa_i)^{\mu_i}\mu_i^{\mu_i}}{\Gamma(\mu_i)(m_i+\kappa_i\mu_i)^{m_i}} \times \prod_{i=1}^{n}\left[(1+\kappa_i)\mu_i\right]^{\mu_1-\mu_i+g_1-g_i} \times \prod_{i=1}^{n}\frac{(m_i)_{g_i}}{(\mu_i)_{g_i}g_i!}\left[\frac{\mu_i^2\kappa_i(1+\kappa_i)}{(m_i+\kappa_i\mu_i)}\right]^{g_i}. \tag{21}$$

The meanings of the parameters in formulas (20) and (21) mentioned above are as follows. m_i, μ_i, and κ_i are all parameters of the κ-μ shadowed distribution. m_i are the shaping parameters of Nakagami-m random variables, μ_i are non-negative natural numbers, representing the number of clusters, and κ_i are non-negative real numbers, expressing the ratio of overall power of the primary ingredients to aggregate power of the dispersive waves. In addition, g_i means loop variables, n represents the number of cascade, and $G_{p,q}^{m,n}[\cdot]$ is Meijer's G function [39].

4. Analysis of OP and IP

In this section, we mainly research the accurate expressions of OP and IP based on the above channel model and statistical properties of multi-cascade κ-μ shadowed fading.

4.1. Outage Probability. OP is the probability that the instantaneous SNR of the system output is lower than a fixed threshold; the threshold is γ_{th}; then, the expression of OP is

$$P_{\text{out}} = P_\gamma(\gamma \le \gamma_{\text{th}}) = F_\gamma(\gamma_{\text{th}}). \tag{22}$$

Substituting (20) into (22),

$$P_{\text{out}} = \sum_{g_1=0}^{\infty}\sum_{g_2=0}^{\infty}\cdots\sum_{g_n=0}^{\infty}\frac{\Lambda_x}{2}\left(\frac{\gamma_{\text{th}}}{\overline{\gamma}}\right)^{\mu_1+g_1} \times G_{1,n+1}^{n,1}\left[\frac{\prod_{i=1}^{n}(1+\kappa_i)\mu_i}{\overline{\gamma}}\gamma_{\text{th}}\middle|\begin{matrix}1-\mu_1-g_1\\ \zeta\end{matrix}\right]. \tag{23}$$

4.2. Intercept Probability. IP is expressed as the probability that the eavesdropping channel capacity is greater than the target secrecy rate, which is the probability of the system being eavesdropped. Then, the IP can be presented as

$$P_{\text{int}} = P(C_E > R_S) = 1 - P(C_E \le R_S) = 1 - F_\gamma\left(e^{R_S}-1\right), \tag{24}$$

where we suppose that C_E represents the channel capacity of the eavesdropping and R_S is the target secrecy rate; substituting (20) into (24),

$$P_{\text{int}} = 1 - \sum_{g_1=0}^{\infty}\sum_{g_2=0}^{\infty}\cdots\sum_{g_n=0}^{\infty}\frac{\Phi_x}{2}\left(\frac{e^{R_S}-1}{\overline{\gamma}}\right)^{\mu_1+g_1} \times G_{1,n+1}^{n,1}\left[\frac{\prod_{i=1}^{n}(1+\kappa_i)\mu_i}{\overline{\gamma}}\left(e^{R_S}-1\right)\middle|\begin{matrix}1-\mu_1-g_1\\ \zeta\end{matrix}\right]. \tag{25}$$

5. Numerical Analysis

In this section, some comparisons between numerical simulation results and Monte Carlo trials are provided. All experimental figures show that the theoretical results are consistent with the simulation trials. In Figures 2–6, unless otherwise mentioned, we used the following parameter settings: $m_1 = m_2 = 1$, $\kappa_1 = \kappa_2 = 2$, $\mu_1 = \mu_2 = 2$, $C_{\text{th}} = 1$, and $n = 2$. It is worth noting that although the derived formulas contain infinite series, it has been verified by simulation that the expressions of OP and IP have converged when the number of simulation cycles reaches 50.

Figure 2 demonstrates the OP and IP versus the average SNR in different cascade numbers ($n = 1, 2, 3$). It can be observed that the influence of the cascade degree n on the value of IP varies with the change of the average SNR. When $\overline{\gamma} > 2$ dB, as n increases, the IP gradually decreases. Also, when the SNR is large, increase in n will enhance its security. The value of OP becomes bigger with the increase of n, which may be due to the increase in the number of scatterers between the transmitter and the receiver, which reduces the possibility of successful transmission.

Figure 3 presents the impact of OP and IP with average SNR in different parameters ($\kappa = 1, 2, 3$). We clearly see that the Monte Carlo simulations and theoretical curves coincide very well. Comparing Figures 3 and 2, it can be concluded that the trends of their diagrams are similar, and the influences of cascade degree n and the parameter κ on OP and IP are analogical. However, the change amplitude of OP and IP caused by different n values is more significant than that caused by different κ.

Figure 4 plots the variation of OP and IP with average SNR in different thresholds ($C_{\text{th}} = 1, 2, 3$). We can note that in the entire range of the abscissa, as the SNR rises, the reliability of the system increases while the security decreases. Furthermore, as the value of C_{th} increases, OP rises and IP reduces. Therefore, the reliability of the channel will decrease by increasing the threshold, and the anti-eavesdropping capability of the channel will be improved.

Figure 5 depicts the OP and IP versus the average SNR when m is different. The figure presents that when $\overline{\gamma} > 2$ dB, OP reduces and IP increases with the increase of m, which shows that when $\overline{\gamma} > 2$ dB, the increase of parameter m will strengthen the reliability of the multi-cascade network, and its security will gradually worsen with the increase of m. When $\overline{\gamma} < 2$ dB, the change of m has little impact on the reliability, and the security improves with the increase of the value of m.

Figure 6 illustrates the OP and IP versus average SNR in different parameters ($\mu = 1, 2, 3$). The figure shows that as the average SNR increases, OP decreases and IP rises. It means that increasing the average SNR can improve the reliability and weaken its security. Through the analysis of Figures 6 and 5, we discover that the various tendencies of

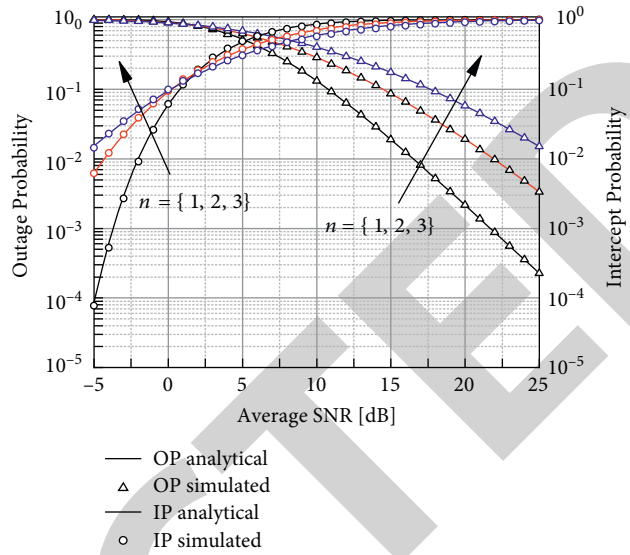

Figure 2: OP and IP versus average SNR for various values of n.

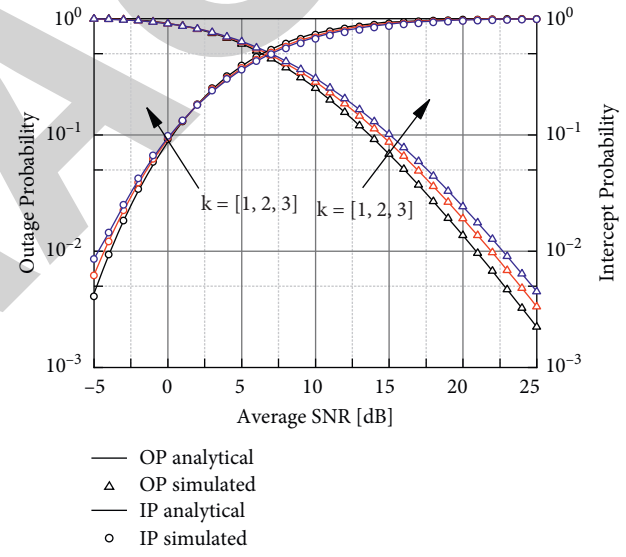

Figure 3: OP and IP versus average SNR for various values of κ.

the two figures are similar, which shows that the changes of the parameters m and μ of the system have similar effects on the communication process of the multi-cascaded κ-μ shadowed fading channels.

In summary, the parameters of the channel and the environmental parameters in the model determine the transmission and security performance. Utilizing Figures 2–6, we can obtain the settings for enhanced security performance as smaller cascade degree n, small SNR, large threshold C_{th}, and small κ and m and the environmental settings for improving the transmission performance as larger SNR, small threshold, small cascade degree, and large m and μ at low SNR.

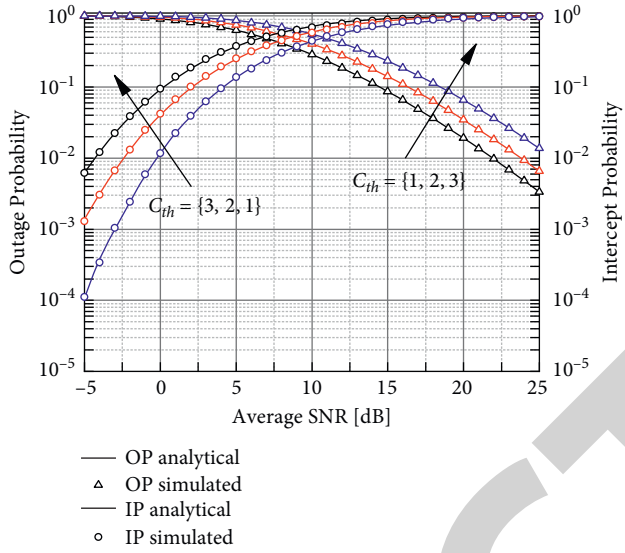

Figure 4: OP and IP versus average SNR for various values of C_{th}.

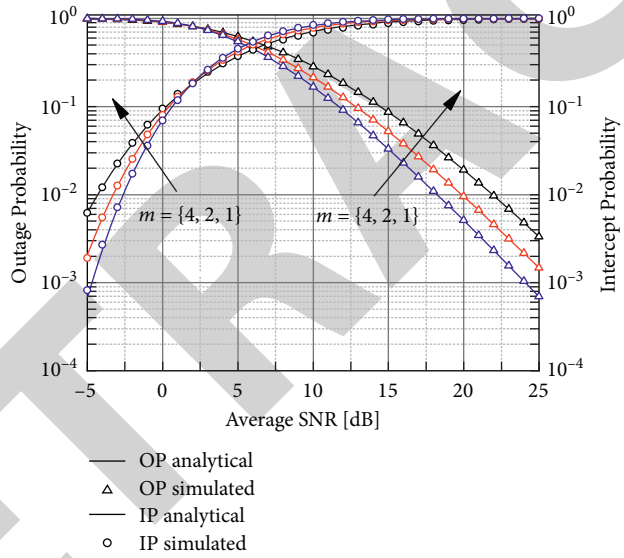

Figure 5: OP and IP versus average SNR for various values of m.

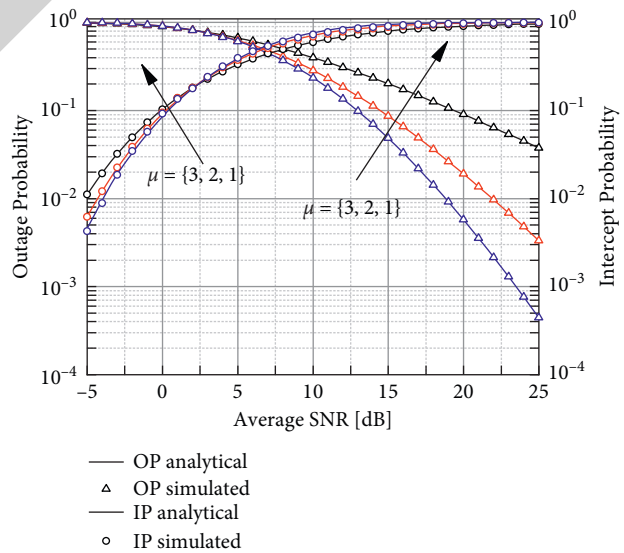

Figure 6: SOP OP and IP versus average SNR for various values of μ.

6. Conclusion

This paper mainly studies the n-level cascade situation of the κ-μ shadowed fading under Wyner's eavesdropping model. In particular, the statistical characteristics including the PDF and CDF of the amplitude and SNR are investigated. Then, the evaluation indicators (OP and IP) are obtained. Finally, we conduct theoretical simulations and Monte Carlo trials, respectively. According to the simulation results, we analyze the factors that affect the reliability and security. In addition, the multi-cascade system studied in this article can provide a theoretical basis for vehicle-to-vehicle communication and satellite communication systems.

Appendix

Utilizing the formula [30]

$$ {}_1F_1(a;b;x) = \sum_{n=0}^{\infty} \frac{(a)_n}{(b)_n n!} x^n, \tag{A.1} $$

we can obtain

$$ {}_1F_1\left(m_1;\mu_1;\frac{\mu_1^2\kappa_1(1+\kappa_1)(y/t)^2}{\Omega_1(m_1+\kappa_1\mu_1)}\right) = \sum_{g_1=0}^{\infty} y^{2g_1} t^{-2g_1} \frac{(m_1)_{g_1}}{(\mu_1)_{g_1} g_1!} \left[\frac{\mu_1^2\kappa_1(1+\kappa_1)}{\Omega(m_1+\kappa_1\mu_1)}\right]^{g_1}, \tag{A.2} $$

and

$$ {}_1F_1\left(m_2;\mu_2;\frac{\mu_2^2\kappa_2(1+\kappa_2)(t)^2}{\Omega_2(m_2+\kappa_2\mu_2)}\right) = \sum_{g_2=0}^{\infty} t^{2g_2} \frac{(m_2)_{g_2}}{(\mu_2)_{g_2} g_2!} \left[\frac{\mu_2^2\kappa_2(1+\kappa_2)}{\Omega_2(m_2+\kappa_2\mu_2)}\right]^{g_2}. \tag{A.3} $$

According to [37, 39], we have

$$ \exp(-\mathrm{px}) = G_{0,1}^{1,0}\left[\mathrm{px}\middle|\begin{matrix}-\\0\end{matrix}\right], \tag{A.4} $$

$$ G_{u,v}^{s,t}\left[x^{-1}\middle|\begin{matrix}c_p\\d_q\end{matrix}\right] = G_{v,u}^{t,s}\left[x\middle|\begin{matrix}1-d_q\\1-c_p\end{matrix}\right]. \tag{A.5} $$

Using (A.4) and (A.5), we get

$$ \exp\left[-\frac{(1+\kappa_1)\mu_1}{\Omega_1} y^2 \eta^{-1}\right] = G_{0,1}^{1,0}\left[\frac{(1+\kappa_1)\mu_1}{\Omega_1} y^2 \eta^{-1}\middle|\begin{matrix}-\\0\end{matrix}\right] = G_{1,0}^{0,1}\left[\frac{\Omega_1}{(1+\kappa_1)\mu_1 y^2}\eta\middle|\begin{matrix}1\\-\end{matrix}\right], \tag{A.6} $$

and

$$ \exp\left[-\frac{(1+\kappa_2)\mu_2}{\Omega_2}\eta\right] = G_{0,1}^{1,0}\left[\frac{(1+\kappa_2)\mu_2}{\Omega_2}\eta\middle|\begin{matrix}-\\0\end{matrix}\right]. \tag{A.7} $$

Substituting (A.2), (A.3), (A.6), and (A.7) into (7) and using variable substitution, the following formula can be obtained:

$$ \begin{aligned} f_{Y_2}(y) = {} & \sum_{g_1=0}^{\infty}\sum_{g_2=0}^{\infty} \frac{\Phi_1\Phi_2}{2} y^{2\mu_1+2g_1-1} \times \int_0^{\infty} \eta^{-\mu_1+\mu_2-g_1+g_2-1} \\ & \times G_{0,1}^{1,0}\left[\frac{(1+\kappa_2)\mu_2}{\Omega_2}\eta\middle|\begin{matrix}-\\0\end{matrix}\right] \times G_{1,0}^{0,1}\left[\frac{\Omega_1}{(1+\kappa_1)\mu_1 y^2}\eta\middle|\begin{matrix}1\\-\end{matrix}\right] d\eta\,. \end{aligned} \tag{A.8} $$

Then, use the classical integrals of the two Meijer's G functions given in [39]:

$$\int_0^{\infty} \tau^{\alpha-1} G_{u,v}^{s,t}\left[w\tau \middle| \begin{matrix} a_1,\ldots,a_t,a_{t+1},\ldots,a_u \\ \kappa_1,\ldots,\kappa_s,\kappa_{s+1},\ldots,\kappa_v \end{matrix}\right] G_{p,q}^{m,m}\left[\sigma\tau \middle| \begin{matrix} e_1,\ldots,e_n,e_{n+1},\ldots,e_p \\ f_1,\ldots,f_m,f_{m+1},\ldots,f_q \end{matrix}\right] d\tau$$
$$= w^{-\alpha} G_{v+p,u+q}^{m+t,n+s}\left[\frac{\sigma}{w} \middle| \begin{matrix} e_1,\ldots,e_n,1-\alpha-\kappa_1,\ldots,1-\alpha-\kappa_s,1-\alpha-\kappa_{s+1},\ldots,1-\alpha-\kappa_v,e_{n+1},\ldots,e_p \\ f_1,\ldots,f_m,1-\alpha-a_1,\ldots,1-\alpha-a_t,1-\alpha-a_{t+1},\ldots,1-\alpha-a_{u,}f_{m+1},\ldots,f_q \end{matrix}\right]. \tag{A.9}$$

Substitute (A.8) into (A.9) to obtain (9).

Data Availability

The data supporting the results of this study can be obtained from the corresponding author upon request.

Conflicts of Interest

The authors declare that they have no conflicts of interest to report regarding the present study.

Acknowledgments

This study was supported in part by the Key Scientific Research Projects of Higher Education Institutions in Henan Province under grant no. 20A510007 and in part by the Doctoral Fund of Henan Polytechnic University under grant no. B2022-13.

References

[1] A. D. Wyner, "The wire-tap channel," *Bell System Technical Journal*, vol. 54, no. 8, pp. 1355–1387, 1975.

[2] J.-H. Lee, "Full-duplex relay for enhancing physical layer security in multi-hop relaying systems," *IEEE Communications Letters*, vol. 19, no. 4, pp. 525–528, Apr 2015.

[3] H. He and P. Ren, "Secure ARQ protocol for wireless communications: performance analysis and packet coding design," *IEEE Transactions on Vehicular Technology*, vol. 67, no. 8, pp. 7158–7169, 2018.

[4] K. Cao, B. Wang, H. Ding, L. Lv, J. Tian, and F. Gong, "On the security enhancement of uplink NOMA systems with jammer selection," *IEEE Transactions on Communications*, vol. 68, no. 9, pp. 5747–5763, 2020.

[5] A. Yener and S. Ulukus, "Wireless physical-layer security: lessons learned from information theory," *Proceedings of the IEEE*, vol. 103, no. 10, pp. 1814–1825, 2015.

[6] S. Wenbo, "Research on physical layer security schemes based on cooperative wireless communication," in *Proceedings of the 2015 Seventh International Conference on Measuring Technology and Mechatronics Automation*, pp. 888–891, IEEE, Nanchang, China, 13 June 2015.

[7] J. Barros and M. R. D. Rodrigues, "Secrecy capacity of wireless channels," in *Proceedings of the 2006 IEEE International Symposium on Information Theory*, pp. 356–360, IEEE, Washington, USA, 9 July 2006.

[8] M. Bloch, J. Barros, M. R. D. Rodrigues, and S. W. McLaughlin, "Wireless information-theoretic security," *IEEE Transactions on Information Theory*, vol. 54, no. 6, pp. 2515–2534, 2008.

[9] A. Goldsmith, *Wireless Communications*, Vol. 10, Cambridge University Press, Cambridge, UK, Aug 2005.

[10] M. K. Simon and M.-S. Alouini, *Digital Communication over Fading Channels*, Vol. 95, Wiley, Hoboken, NJ, USA, 2005.

[11] L. Mason, "Error probability evaluation for systems employing differential detection in a Rician fast fading environment and Gaussian noise," *IEEE Transactions on Communications*, vol. 35, no. 1, pp. 39–46, Jan 1987.

[12] S. O. Rice, "Statistical properties of a sine wave plus random noise," *Bell System Technical Journal*, vol. 27, no. 1, pp. 109–157, Jan 1948.

[13] H. Popovic, D. Stefanovic, A. Mitic, I. Stefanovic, and D. Stefanovic, "Some statistical characteristics of Nakagami-m distribution," in *Proceedings of the 2007 8th International Conference on Telecommunications in Modern Satellite, Cable and Broadcasting Services*, pp. 509–512, IEEE, Serbia, Nis, 26 September 2007.

[14] M. Yacoub, "The η-μ distribution: a general fading distribution," in *Proceedings of the Vehicular Technology Conference Fall 2000. IEEE VTS Fall VTC2000. 52nd Vehicular Technology Conference*, vol. 2, pp. 872–877, IEEE, Boston, MA, USA, 24 September 2000.

[15] M. Daoud Yacoub, "The α-μ distribution: a general fading distribution," *The 13th IEEE International Symposium on Personal Indoor and Mobile Radio Communications*, vol. 2, pp. 629–633, 2002.

[16] X. Li, J. Li, Y. Liu, Z. Ding, and A. Nallanathan, "Residual transceiver hardware impairments on cooperative NOMA networks," *IEEE Transactions on Wireless Communications*, vol. 19, no. 1, pp. 680–695, Jan 2020.

[17] M. Yacoub, "The κ-μ distribution: a general fading distribution,"vol. 3, pp. 1427–1431, in *Proceedings of the IEEE 54th Vehicular Technology Conference. VTC Fall 2001*, vol. 3, pp. 1427–1431, IEEE, Atlantic City, NJ, USA, 7 October 2001.

[18] X. Li, J. Li, and L. Li, "Performance analysis of impaired swipt NOMA relaying networks over imperfect Weibull channels," *IEEE Systems Journal*, vol. 14, no. 1, pp. 669–672, Mar 2020.

[19] F. Gong, J. Ge, and N. Zhang, "SER analysis of the Mobile-Relay-Based M2M communication over double Nakagami-m fading channels," *IEEE Communications Letters*, vol. 15, no. 1, pp. 34–36, Jan 2011.

[20] N. Hajri, N. Youssef, and M. Patzold, "A study on the statistical properties of double Hoyt fading channels," in *Proceedings of the 2009 6th International Symposium on Wireless*

Communication Systems, pp. 201–205, IEEE, Siena, Italy, 7 September 2009.

[21] A. Bekkali, S. Zou, A. Kadri, M. Crisp, and R. Penty, "Performance analysis of passive UHF RFID systems under cascaded fading channels and interference effects," *IEEE Transactions on Wireless Communications*, vol. 14, no. 3, pp. 1421–1433, 2015.

[22] A. Bhowal and R. S. Kshetrimayum, "Large scale MIMO performance analysis over cascaded α-μ MIMO channel for M2M communication," in *Proceedings of the 2017 9th International Conference on Communication Systems and Networks (COMSNETS)*, pp. 405-406, IEEE, Bengaluru, India, 4 January 2017.

[23] Y. Alghorani, G. Kaddoum, S. Muhaidat, S. Pierre, and N. Al-Dhahir, "On the performance of multihop-intervehicular communications systems over n×Rayleigh fading channels," *IEEE Wireless Communications Letters*, vol. 5, no. 2, pp. 116–119, 2016.

[24] G. K. Karagiannidis, N. C. Sagias, and P. T. Mathiopoulos, "$N{\ast}$Nakagami: a novel stochastic model for cascaded fading channels," *IEEE Transactions on Communications*, vol. 55, no. 8, pp. 1453–1458, 2007.

[25] N. C. Sagias and G. S. Tombras, "On the cascaded Weibull fading channel model," *Journal of the Franklin Institute*, vol. 344, no. 1, pp. 1–11, 2007.

[26] D. H. Tashman, W. Hamouda, and I. Dayoub, "Secrecy analysis over cascaded $\kappa -\mu$ fading channels with multiple eavesdroppers," *IEEE Transactions on Vehicular Technology*, vol. 69, no. 8, pp. 8433–8442, 2020.

[27] J. F. Paris, "Statistical characterization of $\kappa{ - }\mu$ shadowed fading," *IEEE Transactions on Vehicular Technology*, vol. 63, no. 2, pp. 518–526, Feb 2014.

[28] J. Sun, X. Li, M. Huang, Y. Ding, J. Jin, and G. Pan, "Performance analysis of physical layer security over shadowed fading channels," *IET Communications*, vol. 12, no. 8, pp. 970–975, 2018.

[29] J. Yang, X. Wu, K. P. Peppas, and P. T. Mathiopoulos, "Capacity analysis of power beacon-assisted energy harvesting MIMO system over $\kappa -\mu$ shadowed fading channels," *IEEE Transactions on Vehicular Technology*, vol. 70, no. 11, pp. 11869–11880, 2021.

[30] B. M. ElHalawany, F. Jameel, D. B. da Costa, U. S. Dias, and K. Wu, "Performance analysis of downlink NOMA systems over κ-μ shadowed fading channels," *IEEE Transactions on Vehicular Technology*, vol. 69, no. 1, pp. 1046–1050, 2020.

[31] M. R. Bhatnagar, "On the sum of correlated squared $\kappa-\mu$ shadowed random variables and its application to performance analysis of MRC," *IEEE Transactions on Vehicular Technology*, vol. 64, no. 6, pp. 2678–2684, 2015.

[32] A. Hussain, S.-H. Kim, and S.-H. Chang, "Dual-Hop Variable-Gain Af relaying with beamforming over κ-μ shadowed fading channels," in *Proceedings of the 2016 IEEE Global Communications Conference (GLOBECOM)*, pp. 1–6, IEEE, Washington, DC, USA, 4 December 2016.

[33] J. Sun, H. Bie, and X. Li, "Security performance analysis of SIMO relay systems over composite fading channels," *KSII Transactions on Internet and Information Systems*, vol. 14, no. 6, pp. 1–6, Jun 2020.

[34] X. Li, J. Li, L. Li, J. Jin, J. Zhang, and D. Zhang, "Effective rate of MISO systems over $\kappa $ - $\mu $ shadowed fading channels," *IEEE Access*, vol. 5, pp. 10605–10611, 2017.

[35] J. Zhang, X. Chen, K. P. Peppas, X. Li, and Y. Liu, "On high-order capacity statistics of spectrum aggregation systems over $\kappa $ - $\mu $ and $\kappa $ - $\mu $ shadowed fading channels," *IEEE Transactions on Communications*, vol. 65, no. 2, pp. 935–944, Feb 2017.

[36] I. S. Gradshteyn and I. M. Ryzhik, *Table of Integrals, Series, and Products*, Academic, New York, NY, USA, 7th ed edition, 2007.

[37] N. Simmons, C. R. N. D. Silva, S. L. Cotton, P. C. Sofotasios, S. K. Yoo, and M. D. Yacoub, "On shadowing the κ-μ fading model," *IEEE Access*, vol. 8, pp. 120513–120536, 2020.

[38] V. S. Adamchik and O. I. Marichev, "The algorithm for calculating integrals of hypergeometric type functions and its realization in reduce system," in *Proc. Int. Symp. Symbolic Algebric Comput*, pp. 212–224, ACM, Tokey, Japan, 1990.

[39] "Wolfram research," https://functions.wolfram.com/HypergeometricFunctions/MeijerG/ accessed.